



# PERFORMANCE OF GA BASED DFIG WITH WPGS IN STANDALONE MODE

(Bukya Anupama <sup>1</sup> Dr.E.Kiran Kumar <sup>2</sup>)

<sup>1</sup>(M.Tech Student, Dept. of Electrical and Electronics Engineering, Swetha Institute of  
Technology and Science, India)

Email Id: bukyaanupama03@gmail.com

<sup>2</sup>(Professor, Dept. of Electrical and Electronics Engineering, Swetha Institute of Technology and  
Science, India)

Email Id: endala.kirankumar@gmail.com

## Abstract:

This paper proposes a Performance of GA based DFIG with WPGS in Standalone mode procedure for a breeze turbine driven doubly fed induction generator (DFIG) with a battery energy accumulating (BES) in independent mode. The proposed control plot has multi-functionalities, for instance, disposal music, compensation of lopsided weight streams and extraction of most prominent power from the breeze. The control of rotor side converter and liad side converter, relies upon field arranged philosophy. The proposed GA based control has incredible amazing response when stood out from customary control figurings. The tip speed extent based most prominent power point following technique is used to isolate most extraordinary power from the breeze. The entertainment of DFIG based breeze power age structure (WPGS) is finished under various conditions, for instance, steady wind speed, variable breeze speeds and weight streams unbalancing using Simpower Systems device compartment of MATLAB. The DFIG stator voltages and streams are found changed and sinusoidal by keeping up steady repeat and voltage at PCC.

keywords--WPGS, DFIG, battery energy storage (BES), fuzzy logic control (FLC), MPPT.

## 1. INTRODUCTION:

Attributable to use of non-renewable energy source for power age, some unfriendly impacts are seen on the earth, for example, ozone depleting substance, corrosive downpour, ozone layer consumption and a worldwide temperature alteration [1]. To adjust between power age and force utilization, a local force age must be started in the

dissemination system to keep the atmosphere clean and to take care of the neighborhood loads. These days, the approaches for inexhaustible force age bolster the capital appropriations to elevate its applications and to give sponsorships in charges [2]. The utilization of sustainable power sources (RES) in the conveyance framework, is blasting in the creating nations because of market entrance, learning expertise and developing advances. These days, little scope RES are introduced in family structures, business structures, water systems, ventures, human services administrations, and so on. In addition, a few favorable circumstances of RES, are referenced as follows.

Inexhaustible force age is eco-accommodating as it produces no loss during activity and having immaterial commitment in nursery impacts, corrosive downpours and so on. In this manner, environmentally friendly power vitality sources are sans contamination and have insignificant effect on nature.

The RES has low working cost, low upkeep cost as it is openly accessible with unlimited regular asset.

Among the sensible power sources, the specialists have discovered the all-inclusive idea toward wind centrality due to developments in The financial viewpoints of wind turbines [3]-[5]. Wind turbines are overwhelmingly coordinated as fixed and variable velocity forms. As a result of their insistence and openness on job highlights, prior fixed speed wind turbinen have been used, a clear share of power in the indistinguishable is at any rate squandered [4]. Thus, the double-taken care of the DFIG generator



and fluctuating wind turbines for the production have been extended around the world. The use of DFIG with wind turbines, when it stands apart from geographies with steady generators of speed as stated in [7], has different focal centers [8] as,

- The converter rating is reduced in view of the way it slips the stator control.
- The DFIG is fundamentally centrality skilled and has less force catastrophes.
- It makes less acoustic commotion.
- Most generally, it is remarkably fitting for variable speed development, which is expected to get top force, particularly during differentiating breeze conditions.

Authorisation and organisational planning strategies are available in a low-power era setting with wind turbine combination DFIG (WPGS). The cross-segment-related DFIG-based WPGS has been considerably scrutinized [7],[8]. In [7] it is not compelling to track the frame power stream, because DFIG is not provided to a side converter. Furthermore, the force efficiency viewpoints of the usefulness in the equivalent are not discussed. In [8] DFIG's models have struggled with mutilated network voltage to introduce fair regulated methods. It has a high calculational weight, a high flexibility and a high basic memory. For small association voltages, a sliding mode-based control plot has been depicted in [9]. As the sliding mode controller allows difficult exchange rates, the VSC presence time is decreased.

Regardless, the extent of examination on free DFIG based WPGS isn't conspicuous and analyzed. In self-sufficient methodology for activity, it is particularly fundamental to keep up solid rehash, reliable voltage at load end near to the music inside very far [10]. The control plans for both rotor side converter (RSC) and weight side converter (LSC) of DFIG, are appeared with a definitive target that the as of late referred to targets are developed.

There are different most vital force point following (MPPT) procedures in the making [11], [12] to ensure about pinnacle power from the breeze. Notwithstanding, tip speed degree This thesis uses the MPPT method. The value of battery repayment (BES) unambiguously expects a main occupation with an autonomous strategy for the activities of DFIG. The way to charge the flood power to BES is considered, provided lower interest at high wind speeds. In this case BES supplies the offset power with a definitive goal for the MPPT breeze turbine

generator to be used in case the stack requirement is high and the wind speed is low. In [13],[14] a portion of DFIG's self-reliance framework for BES is provided. Mendis et al. [14] tested the free bidirectional DFIG-associated BES at the DC interface. By the by, different relative essential controllers (PICs) make the control calculation of when in doubt structure complex what's more, it comes up short on the test underwriting.

The basic duty of this assessment, contains striking attributes of the control assessments, which are as indicated by the going with.

- The single information variable managed FLC is utilized to tune PIC of terminal voltage at PCC by utilizing LSC and PIC of speed control for MPPT development utilizing RSC, which has less computational weight and memory basic.
- Both RSC and LSC control tallies are made utilizing stator change masterminded theory.
- The centrality storing up contraption is really added at DC relationship of two VSCs related progressive, which helps in dealing with and giving equity power in phenomenal working states of DFIG based WPGS.
- The DFIG stator streams, PCC voltages are changed and sinusoidal, which join the sounds inside the IEEE-519 norm.

- The terminal voltage at PCC and its rehash, are kept up steady during dynamic conditions, for example, ariable breeze speed, load unbalancing, and so on

The DFIG based WPGS in autonomous mode dealing with threephase, four wire loads, is shown and reproduced using SimPowerSystems toolbox of MATLAB. The clarifications for the not interfacing neutral wire to the stator of the doubly dealt with acknowledgment generator (DFIG) are according to the accompanying. The generator streams are sinusoidal and changed, which are continually taken thought by the control of weight side converter (LSC). What's more, the neutral wire is needed to pass on ability to the single stage loads (models: house loads, business loads, little extension current weights) and imbalanced close by loads. In the proposed structure, the transformer gives unprejudiced wire to pass on ability to the recently referenced sort of imbalanced and single stage loads. In the proposed geology, the pile side converter

supplies the non-pivotal parts and imbalanced fragments of neighborhood loads, which are related at reason for customary coupling. Also, for the confirmation viewpoint, the power age structure in the power plant, is three-stage three-wire to generate changed power [23-24].

The apex power from the breeze, is gotten by using tip speed extent MPPT system. Using a made model, the reliable state and transient displays are poor down in detail..

## 2.1 SYSTEM CONFIGURATION:

The photo. 1 shows WPGS based on DFIG, transmitted in a self-governing measure on a standard pile of 2 kW and a pex stack of 4 kW. The DFIG stator winches supply the pilot with the addition of two back to back VSCs in the rotor windings to the PCC. The VSC, which is similar to the PCC, is called LSC, and the VSC, which is associated with the rotor twist, is called RSC. BES is connected to the standard DC association of two VSCs, as shown in Fig.. In this particular case, the role is addressed in the contrasting paragraphs for each fragment.

### A. Design of Wind Turbine and Gear Mechanism

The wind power captured by the turbine,  $P_m$  is given as ,

$$P_m = 0.5C_p(\lambda, \beta)\rho AV_w^3 = 0.5C_p(\lambda, \beta)\rho\pi r^2 V_w^3 \quad (1)$$

Where,  $\rho$  is air specific density. Which is considered as 1.1514

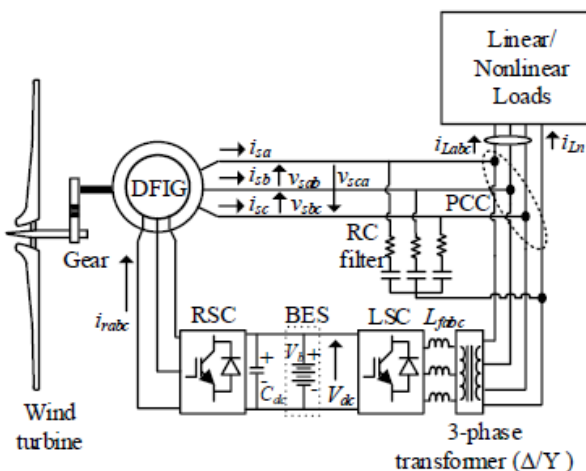


Fig. 1. DFIG based WPGS in standalone mode with BES.

$\text{kg/m}^3$ ;  $V_w$  denotes wind speed in (m/s);  $A$  is a wind turbine blade area occupied in ( $\text{m}^2$ );  $C_p$ , which depending on blade pitch  $\beta$  in (deg) and tip speed ratio

$\alpha$  is called power efficiency (PE) or Turbine coefficient;  $r$  is a wind turbine radius in ( $\text{m}^2$ ) (m).

In [25], the  $C_p$  is given as,

$$C_p(\lambda, \beta) = C_1 \left\{ \left( \frac{C_2}{\lambda_i} \right) - C_3\beta - C_4 \right\} e^{-C_5/\lambda_i} + C_6\lambda \quad (2)$$

$$\text{where, } \frac{1}{\lambda_i} = \frac{1}{\lambda + 0.08\beta} - \frac{0.035}{\beta^3 + 1}$$

$$C_p(\lambda, \beta) = C_1 \left\{ \left( \frac{C_2}{\lambda_i} \right) - C_3\beta - C_4 \right\} e^{-\frac{C_5}{\lambda_i}} + C_6\lambda$$

In addition, it takes into account the constants  $C_1 = 0.5176$ , the constants  $C_2 = 116$ , the constants  $C_3 = 0.05$ , and the constants  $C_5 = 21$  and  $C_6 = 0.0068$ . The pitch angle of the blade is  $\beta = 0^\circ$ , which is held at a constant value.

The relationship of wind velocity with blade tip velocity as,

$$(\lambda, \beta) = \frac{w_T \times r}{V_w} \quad (3)$$

where,  $w_T$  represents the rotational speed of a wind turbine.

In this work, a breeze turbine of 4.81 kW, is planned at 12 m/s appraised wrap speed by thinking about advance up gear system. The structure is to such an extent that  $C_p$  accomplishes a greatest estimation of 0.48 and relating  $w_T$  is of 8.1, which is viewed as ideal incentive for securing top force from the accessible breeze. The breeze turbine span is determined from (1) is 1.8 m.

The DFIG rotor speed  $w_r$  is communicated regarding  $w_T$  and gear proportion  $\eta$

$$w_r = \eta w_T \quad (4)$$

The base and greatest rotor paces of DFIG, are taken as 110 rad/s and 204 rad/s. By (3) and (4),  $\eta$  is determined as 3.77 at 12 m/s, evaluated wind speed and 204 rad/s, rotor speed.

## 2.2. Tip Speed Ratio Wind-MPPT Method

From the speed-power qualities of wind turbine, it is clear that the rotor speed of DFIG needs to shift to remove top force out of accessible breeze speed. The equivalent is cultivated by creating reasonable reference speed for a particular breeze speed. In this work, the tip speed proportion MPPT strategy [16] is utilized. Also, its numerical plan to infer the reference speed is as per the following ,



$w_T = w_r/\eta$  ---(5)  
substituting (5) in (3) result in as,

$$\lambda = \frac{w_r \times r}{\eta \times V_w} \text{ ---(6)}$$

In (6), for  $\lambda = \lambda_{opt}$ ,  $\omega_r$  gives the reference speed  $\omega_r^*$  as,

$$\omega_r^* = \frac{\eta \times \lambda_{opt} \times V_w}{r} \text{ ---(7)}$$

By substituting the respective values in (7), the reference rotor speed is expressed in terms of  $V_w$  as,

$$\omega_r^* = \frac{3.77 \times 8.1 \times V_w}{1.8} \cong 17 \times V_w \text{ ---(8)}$$

### 2.3. Determination of Power Rating for DFIG

The DFIG can convey power, both from the stator and rotor during very coordinated speed activity. Since speed scope of the rotor, is considered between 110 rad/s to 204 rad/s, the relating slip is +30.0% and - 30.0%, individually. The DFIG is chosen to such an extent that it conveys evaluated power at appraised wind speed. At evaluated power condition, DFIG additionally conveys

$$P_{rin} = P_{rs} + P_{rr} = P_{rs} + |s_{rp}|P_{rs} = (1 + |s_{rp}|)P_{rs}$$

$$P_{rs} = \frac{P_{rin}}{(1 + |s_{rp}|)} \text{ ----(9)}$$

where,  $s_{rp}$  speaks to the slip at evaluated force and it is - 0.3. In the wake of subbing this incentive in (9), gives appraised stator power  $P_{rs}$  of 3.7 kW. In this manner, it is acceptable to plan a DFIG with rating of 3.7 kW, in light of the fact that the need of responsive force is taken consideration by the RSC. This is the fundamental preferred position of DFIG..

### 2.4. Design of DC Link Voltage and BES

The rotor voltage achieves a most extreme incentive at a slip of 0.3, in light of the fact that slip times the stator voltage rises to the rotor voltage. For a 415 V framework, the rotor

voltage is resolved as,  $V_{rm} = 0.3 \times 415 = 125$  V. In this way, the DC interface voltage  $V_{dc}$  is acquired with the accompanying connection as,

$$V_{dc} \geq \left( \frac{2\sqrt{2}}{\sqrt{3 \times m}} \right) V_{rm} \text{ ---(10)}$$

where,  $V_{rm}$  is the rotor most extreme voltage;  $m$  is the adjustment list, is chosen as a solidarity. By subbing the qualities in (10), the DC interface voltage is acquired as 204.1 V. In this framework, it is chosen as 240 V, which can be acknowledged utilizing 20 batteries of 12 V each.

As talked about before, the DFIG based WPGS is intended to flexibly for 30 hours at a normal heap of 2 kW. Subsequently, the capacity limit of BES ends up being 60 kWh. The ampere-hour rating of BES, is determined as (60 kWh/240) and comes to be 250 AH. In this manner, a 240 V, 250 AH BES is required for this framework. By and by, a lot of 12 V and 125 AH batteries are accessible, so to accomplish 240 V, 20 batteries are associated in arrangement and to get 250 AH rating, another 20 batteries are associated in corresponding with the past ones..

### 2.5. Design of Transformer and VSCs Rating

The framework is intended for 3-stage, 4-wire dispersion organize, to cook single stage loads, for which a 3-stage transformer is utilized to give an impartial point. Since the selected voltage of the battery is 240 V, the low voltage (LV) winding voltage,  $V_L(LV)$  according to (10) ought to be under 147 V and it is picked to be 125 V. Accordingly, a 5 kVA, 125/415 V delta star transformer is utilized in this framework. The rating of LSC is chosen as 3.7 kVA (greatest stator power yield when the heap is disengaged) and the current rating (rms) of LSC, is determined as,

$$I_{r(LSC)} = \frac{VA_{LSC}}{\sqrt{3} \times V_{L(LF)}} \text{ --- (11)}$$

The current rating of each protected entryway bipolar transistor (IGBT) IIGBT(LSC) in LSC is gotten as,,

$$I_{IGBT(LSC)} = 1.25\{I_{ppr} + I_{LSC}\} \text{ ---(12)}$$

where,  $I_{ppr}$  is top pinnacle current wave of LSC top current  $I_{pLSC}$  and it is viewed as 5%. In this way,  $I_{pLSC} = 17.09 \times 1.414 = 24.16$  A and  $I_{ppr} = 0.05 \times 24.16 = 1.208$  A. By subbing these qualities in (12), gives most extreme current rating of each IGBT as 31.71 A. Hence, a 50 A current rating IGBT is picked.

The IGBT voltage rating relies upon the DC connect voltage. For instance, for a 264 V as a most extreme DC connect voltage, the IGBT voltage rating would be  $1.25 \times 264 = 330$  V. Here a wellbeing edge of 25% is thought of. In this way, a 600 V is picked as IGBT voltage rating.

The benefit of interfacing inductor is determined from the accompanying ,

$$L_f = \frac{\sqrt{3} \times m \times V_{dcm}}{12 \times a \times f_{sw} \times I_{ppr}} \text{ --- (13)}$$

where,  $m$  signifies tweak record;  $a$  speaks to security factor and its run of the mill esteem is 1.2 to shield IGBT from over flows during drifters;  $f_{sw}$  denotes the IGBT exchanging recurrence;  $V_{dcm}$  represents the greatest voltage of DC interface. Subbing these qualities in (13), gives the estimation of 2.63 mH.

The volt ampere (VA) rating of RSC, is based on most extreme genuine and receptive forces stream by means of RSC. The most extreme genuine force streams by means of RSC at  $s_{rp}$  expressed in subsection-C, is determined as,

e control calculation for RSC, is to such an extent that it supplies required polarization current to DFIG. According to machine boundaries, the DFIG draws a slacking responsive intensity of 2.5 kVAR during motoring mode. The equivalent is provided from the rotor side by RSC. The evaluated rotor

receptive force  $Q_{rr}$  at greatest slip, is determined as,,

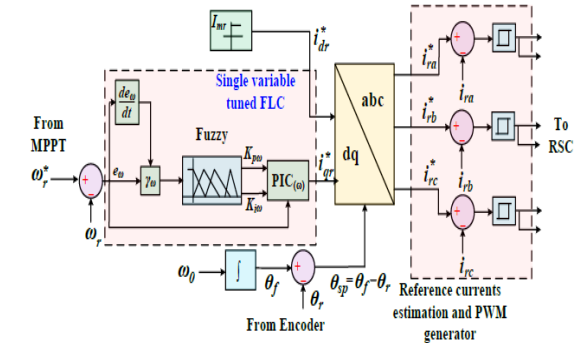


Fig. 2. Control algorithm for RSC.

$$Q_{rr} = s_{rp} \times 2.5 \text{ kVAR} \text{ ---(15)}$$

Now, the overall rating of RSC is computed as,

$$VA_{(RSC)} = \sqrt{P_{rr}^2 + Q_{rr}^2} \text{ ---(16)}$$

Substituting values in (16), gives 1.34 kVA as rating of RSC. Moreover, the current rating of RSC  $I_r(RSC)$  is computed as,

$$I_r(RSC) = \frac{VA_{RSC}}{\sqrt{3} \times V_{rm}} \text{ --- (17)}$$

The current rating of IGBT IIGBT(RSC) in RSC is calculated as,

$$I_{IGBT(RSC)} = 1.25\{(0.05 \times I_{pRSC} + I_{pRSC})\} \text{ ---(18)}$$

where,  $I_{pRSC}$  is the pinnacle current through the RSC, is processed as  $(6.3 \times 1.414 \approx 9$  A) 9 A. Subbing these qualities in (18), gives 11.81 A and its worth is chosen as 50 A. The voltage rating is picked like LSC that is 600 V.

### 3. CONTROL OF RSC AND LSC

These sections discuss control figures for both RSC and LSC. It is shown that a meandering current control is used for both RSC and LSC, and it depends on an approach arranged for stator movement.

#### 3.1. Control Design for RSC

These sections discuss control figures for both RSC and LSC. It is obvious that walking current controls are used for both RSC and LSC and rely on the organised methodology for stator growth.

The key goals of RSC are as seen in the passage.

- Provides a simple voltage age reactive power need for DFIG.
- It controls rotor speeds to conduct MPPT production in any conditions of wind speed.

The photo. 2 RSC control plan diagrams. The short rotor current portion,  $i_{dr}$ , changes along the stator field with the rotor current bit  $i_{qrs}$  with a stage movement of 90 degrees with regard to  $i_{dr}$  in the stator field expected control. Then,  $i_{dr}$  addresses a current part of the open rotor and  $i_{qr}$  addresses assured or limited any part of the rotor current. The power clarification is as,

$$T_e = \left(\frac{3}{2}\right)(p/2)\phi_{sd} i_{qr} \quad \text{---(19)}$$

where,  $\phi_{sd}$  shows the stator progress;  $p$  tends to number of posts of DFIG Due to the fact that  $\phi_{sd}$  is kept the  $q$  part of rotor current  $i_{qr}$  predictable in the field-organized phase, it is truly associated with force. The DFIG rotor speed is subsequently compelled to make a fair reference to  $i_{qr}$ . The speed of reference from MPPT and certified speed, the speed mess up  $e_w$  is for the pic of PIC and the new variable tuned flac weaken, as shown in Figure, are checked and then evaluated. 2. This position is used to change the speed PICs of  $K_{pw}$  and  $K_{iw}$ .

The PIC is used for tracking the DFIG rotor reference speed. Two data factors can perform yield gains in a daily FLC. The more semantic factors in FLC increase the weight, the memory and the nuanced nature of uninterrupted usage. Furthermore, FLC has 2 informative factor, but anyway, a single data variable FLC has one dimensional cushy theory, which is based on a two dimensional feathery. Therefore, an FLC is run by

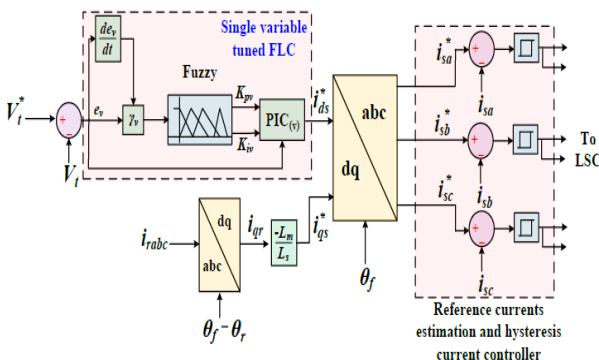


Fig. 5. Control algorithm for LSC.

single info variable is presented. The basic target of this single info variable FLC is that it produces appropriate relative and indispensable additions as the mistake differs. Subsequently, this capacity in the end improves the dynamic execution particularly in accomplishing MPPT in factor wind speed conditions. The speed blunder  $e_0$  and its pace of progress  $(de_0/dt)$ , are applied as contributions to the mistake separation  $e_0$ . This blunder separation is given as contribution to the FLC. The blunder separation is communicated as far as mistake arranges  $(e_0, er_0)$ . Here,  $er_0$  denotes the pace of progress of mistake, the blunder separation for speed control is assessed as,,

$$\gamma_0 = \sqrt{e_0^2 + e_{r_0}^2} \quad \text{---(20)}$$

The Takagi-Sugeno FLC is utilized here to give gains, to appropriately follow the reference speed of DFIG by taking out its blunder as for real speed. Table I and Table II give the fuzzy guidelines to information and yield factors, independently. Here  $Z$  means the etymological worth. The negative high (NH), negative low (NL), little (S), positive low (PL) and positive high (PH), are the estimations of mistake separation. Little (S), medium (M) and high (H), are the estimations of  $K_{pw}$  and  $K_{iw}$ . Fig. 3 and Fig. 4 speak to the enrollment elements of information and yield, separately. The tuned corresponding and basic increases, are applied to PIC of speed to produce reference  $q$  part of rotor  $i_{qr}^*$  as delineated in Fig. 2, is figured as,,

$$i_{q(j)}^* = i_{q(j-1)}^* + K_{pw}(e_w(j) - e_w(j-1)) + K_{iw}e_w(j) \quad \text{---(21)}$$

$$\text{Where, } e_w = \omega_r^* - \omega_r$$

The  $d$  component of rotor reference current [15] is as,

$$i_{dr}^* = I_{mr} = \sqrt{\frac{2}{3}} \left[ \frac{V_f}{X_m} \right] \quad \text{---(22)}$$

where,  $I_{mr}$  is the charging segment of DFIG;  $X_m$  is the polarizing reactance of the machine at base recurrence and  $V_t$  is the terminal voltage.

These reference dq components are changed in to abc coordinates through backwards Park change by methods for point of change  $\theta_{sp}$ . The slip point is registered from the detected rotor edge  $\theta_r$  and fixed



electrical edge  $\theta_f$  at base recurrence  $\omega_0$  in (rad/s) as,,

$$\theta_{sp} = \theta_f - \theta_r \quad \text{---(23)}$$

$$\theta_f = \int_0^t \omega_0 dt$$

The assessed rotor reference flows  $i^*ra$ ,  $i^*rb$ , and  $i^*rc$  are contrasted and detected flows of rotor  $ira$ ,  $irband$   $irc$ , at that point blunder is applied to beat width adjusted control to deliver beats for the IGBT gadgets of RSC.

### B. Control Design for LSC

The fundamental destinations of LSC are as per the following.

- It keeps up steady terminal voltage at PCC by voltage control.
- It bolsters consistent recurrence by utilizing fixed electrical edge as change edge.

Fig. 5 delineates the control strategy of LSC. In LSC control, the reference flows are created for the stator flows of DFIG. The receptive reference some portion of stator current  $i^*ds$ , is assessed by passing terminal voltage blunder through PIC of voltage PIC(V) as appeared in Fig. 5. In this control, increases of PIC are tuned utilizing single information variable FLC as talked about in subsection-A. The enrollment elements of info and yield to follow voltage reference, are given in Fig. 6 and Fig. 7,

separately. The fuzzy standards are like the subsection-A. It is noticed that  $\square v$  speaks to the blunder separation,  $e_v$  denotes voltage mistake and  $(\text{dev} \square / dt)$  demonstrates pace of voltage blunder. The tuned  $K_{pv}$  and  $K_{iv}$  are given to the FLC, which produces  $i^*ds$  as,

$$i^*_{dc(j)} = i^*_{dc(j-1)} + K_{pv}(e_{v(j)} - e_{v(j-1)}) + K_{iv}e_{v(j)} \quad \text{---(24)}$$

$$\text{Where, } e_v = V_t^* - V_t$$

The active reference part of stator current  $i^*q_{s}$  is related with the  $i^*q_{r}$  as follows.

$$i^*_{qs(j)} = -\left(\frac{L_m}{L_s}\right) i^*_{qr} \quad \text{---(25)}$$

The registered dq stator reference flows are changed over back to genuine abc arranges by utilizing reverse Park change with fixed electrical edge as change point, which can be seen from Fig. 5. The reference stator flows  $i^*sa$ ,  $i^*sb$ , and  $i^*sc$  are acquired correlation with detected stator winding flows  $isa$ ,  $isb$  and  $isc$ , at that point the current mistake is applied to the hysteresis band current control, which produces beats for IGBT gadgets inside the LSC..

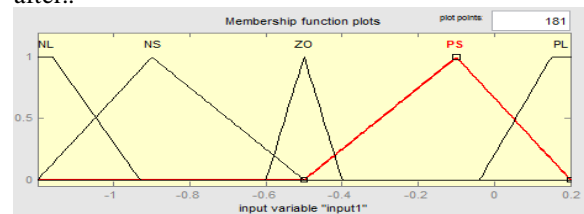
## 4. Fuzzy Logic Controller:

A fuzzy control system is a fuzzy logic control framework, a logical structure which investigates statistical information which is commonly shown as rational parameters that somewhere in the scope of 0 and 1 have consistent characteristics rather than old style or propelled reasoning, dealing with distinct figures of either 1 or 0 (valid or bogus, independently). In computer control, fuzzy logic is used comprehensively. The word 'fuzzy' indicates the manner during which the reasoning included will supervise ideas that can not be expressed as 'true' or 'false' but rather as 'mostly apparent.' Although elective approaches, for example, non-exclusive counts and neural frameworks can function a significant part of the time similarly to fuzzy logic, fuzzy logic has the preferred position that the solution to the problem can be tossed into wording that human directors can see, so their information could be used in the controller's architecture. This makes it less difficult to mechanize tasks that are starting at now viably performed by individuals..

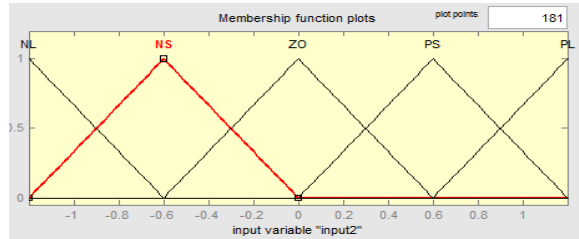
### 4.1 Fuzzy sets:

The data factors in a fuzzy control system are all things considered planned by sets of enlistment limits this way, known as fuzzy sets. The path toward changing over a new data motivation to a fuzzy worth is called 'fuzzification'.

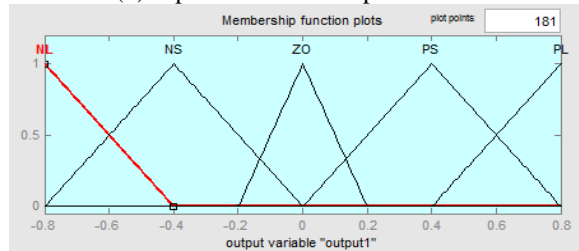
The enlistment components of the Fuzzy controller used in our propagation model are given as seeks after..



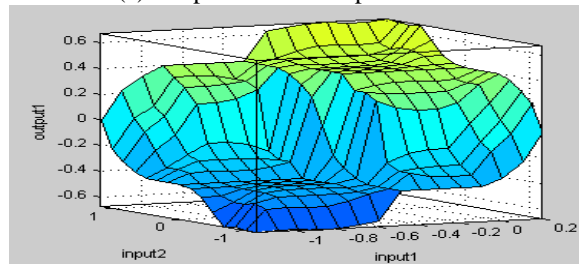
(a) Input 1 Membership Function.



(b) Input 2. Membership Function



(c) Output Membership Function.

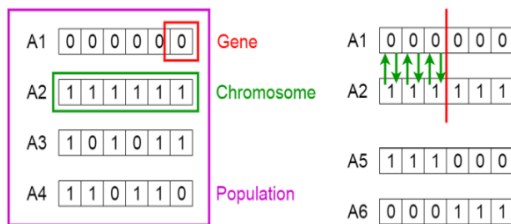


(d) Fuzzy structure

Figure 5. Fuzzy Logic Control

### Genetic algorithm:

A **Genetic** calculation is a request heuristic that is propelled by Charles Darwin's speculation of typical headway. This figuring mirrors the strategy of customary decision where the fittest individuals are picked for augmentation in order to convey any kind of family down the line of individuals to come.



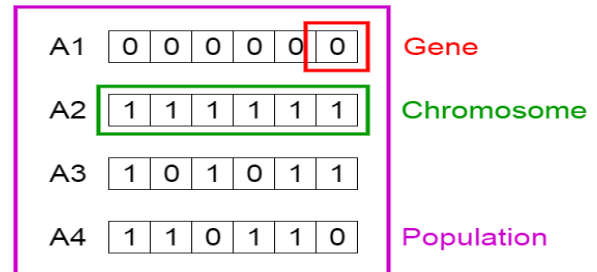
watchmen and have a pervasive possibility at continuing on. This philosophy continues reiterating and toward the end, an age with the fittest people will be found. This idea can be applied for a solicitation issue. We consider a lot of answers for an issue and select the game-plan of best ones out of them.

Five stages are considered in a hereditary calculation.

1. Initial populace
2. Fitness capacity
3. Selection
4. Crossover
5. Mutation

### Initial Population

The method starts with numerous people which is known as a Population. Every individual is a reaction for the inconvenient you need to solve. An individual is portrayed by a lot of cutoff points (factors) known as Genes. Qualities are joined into a string to layout a Chromosome (solution). In an acquired calculation, the arrangement of attributes of an individual is tended to utilizing a string, like a letters all together. Usually, equivalent qualities are utilized (plan of 1s and 0s). We express that we encode the attributes in a chromosome.



Population, Chromosomes and Genes

### Fitness Function

The wellness work dictates just how a person is fit (the capacity of a person to contend with others). Every person receives a wellness score. The probability of a person being preferred for proliferation depends on his wellness results.

### Selection

### Notion of Natural Selection

The procedure of brand name choice beginnings with the confirmation of fittest people from an all inclusive community. They produce any sort of future family which pick up the properties of the guards and will be added to people to come. In the event that guardians have better wellbeing, their family will be superior to

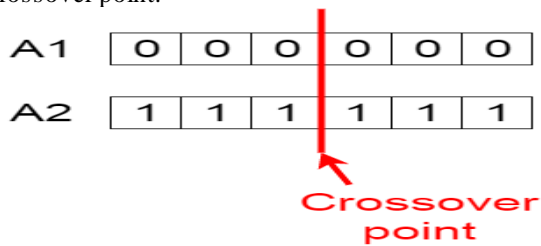




The possibility of determination stage is to choose the fittest people and let them pass their qualities to the following generation. Two sets of people (guardians) are chosen dependent on their wellness scores. People with high wellness have progressively opportunity to be chosen for multiplication.

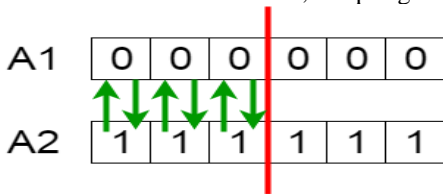
**Crossover**

In hereditary calculations Crossover is the most important step. A hybrid point is selected from within the qualities for every pair of guardians to be paired. For example, take 3 as shown below to consider the crossover point.

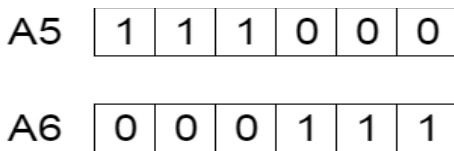


Crossover point

Despite exchange of parents' genes between parents until the crossover is reached, offspring are produced.



Exchanging genes among parents The new offspring are added to the population.

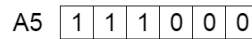


New offspring

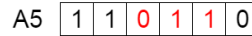
**Mutation**

A part of their qualities may be experiencing changes with a low irregular probability in some newly framed posterities. This means that part of the bits can be reversed in the bit string.

Before Mutation



After Mutation



Change: previously, then after the fact

Transformation happens to hold populace variety and stop untimely intermingling.

**Termination**

The estimation ends when the population has joined together (does not offer posterity that is fundamentally different from the previous age). It is said at that point that the inherited calculation gave us several answers.

**Comments**

The size of the population is fixed. When the new ages are framed, people with the least impressive room have been restated to create people that are superior to the old age. The classification of stage events is re-created.

**Pseudocode**

START  
Generate the initial population  
Compute fitness  
REPEAT  
Selection  
Crossover  
Mutation  
Compute fitness  
UNTIL population has converged  
STOP

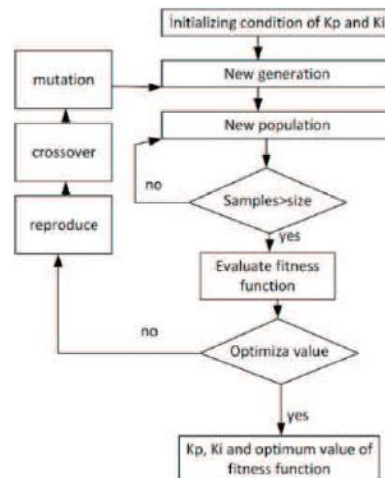


Fig. . Flow chart for STATCOM tuning using GA



### 5.0 Simulation results with FLC:

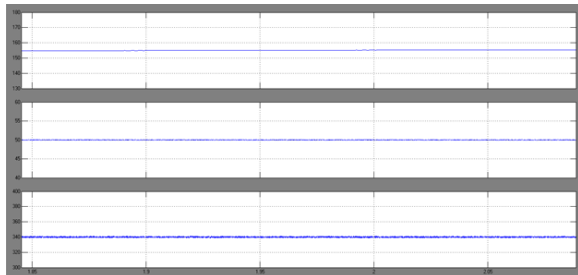
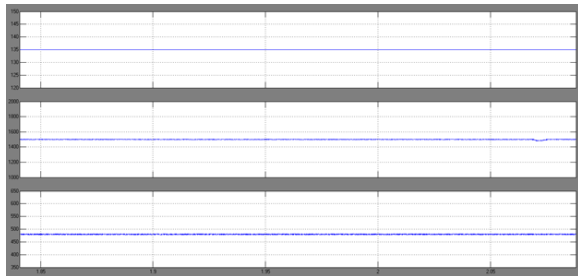
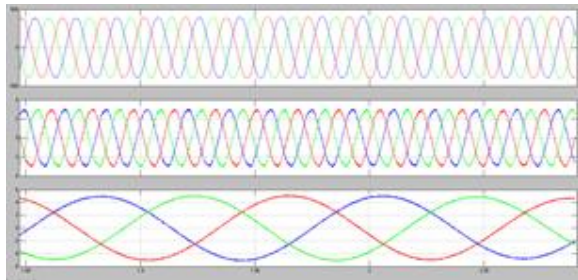
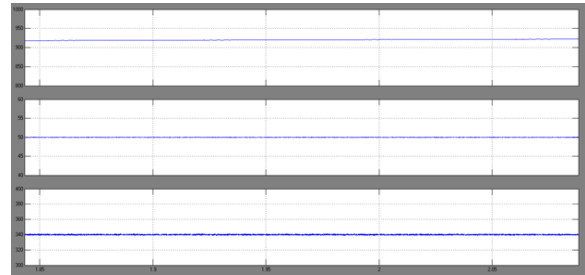
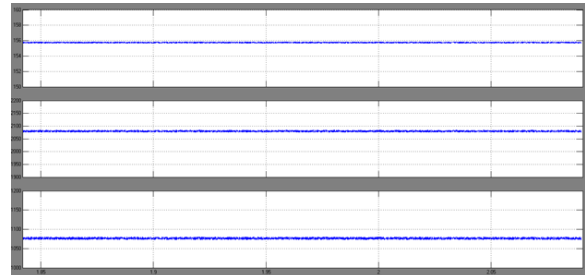
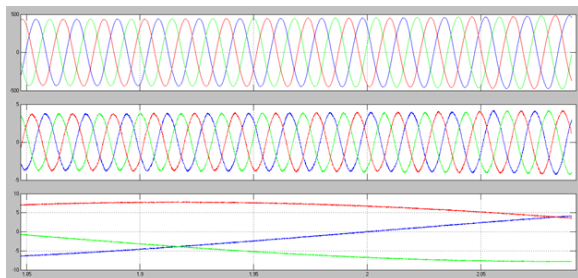


Fig. 8. Performance of the DFIG based WPGS with BES at constant wind speed of (a) 8 m/s (subsynchronous speed of DFIG):  $v_{sabc}$ ,  $i_{sabc}$ ,  $i_{rabc}$ ,  $\omega_r$ ,  $P_s$ ,  $P_LSC$ ,  $P_b$ ,  $V_t$ ,  $f_s$



(b) 9.23 m/s (synchronous speed of DFIG):  $v_{sabc}$ ,  $i_{sabc}$ ,  $i_{rabc}$ ,  $\omega_r$ ,  $P_s$ ,  $P_LSC$ ,  $P_b$ ,  $V_t$ ,  $f_s$ .

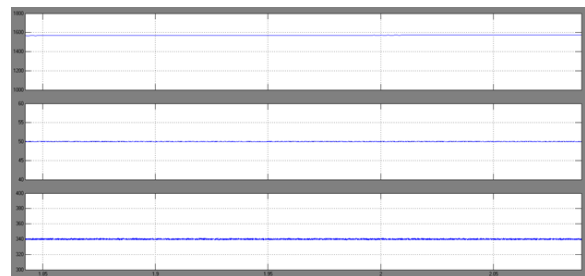
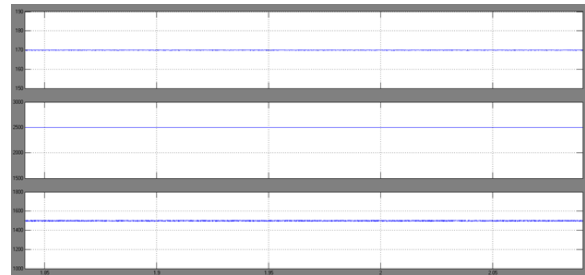
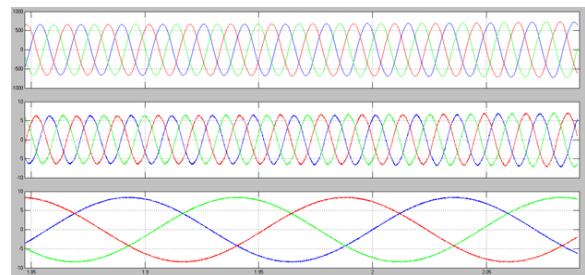
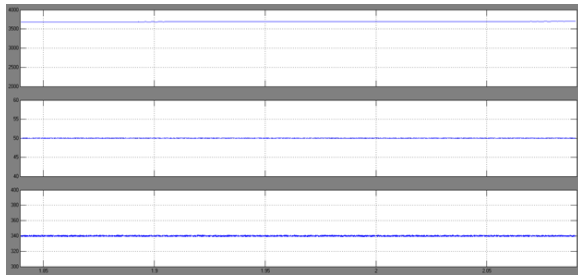
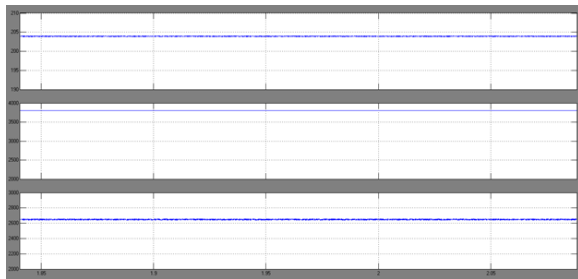
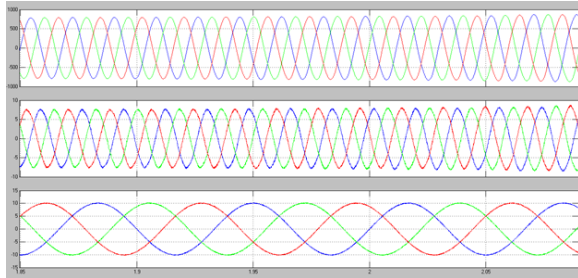


Fig. 9. Performance of the DFIG based WPGS with BES at constant wind speed of (a) 10 m/s



(supersynchronous speed of DFIG):  $v_{sabc}$ ,  
 $i_{sabc}$ ,  $i_{rabc}$ ,  $\omega_r$ ,  $P_s$ ,  $PLSC$ ,  $P_b$ ,  $V_t$ ,  $f_s$



(b) 12 m/s (supersynchronous speed of DFIG):  
 $v_{sabc}$ ,  $i_{sabc}$ ,  $i_{rabc}$ ,  $\omega_r$ ,  $P_s$ ,  $PLSC$ ,  $P_b$ ,  $V_t$ ,  $f_s$ .

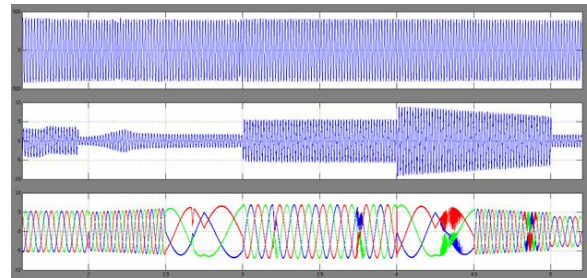
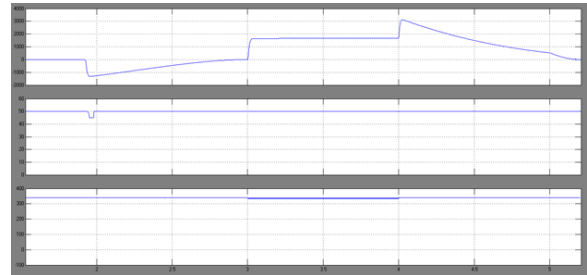
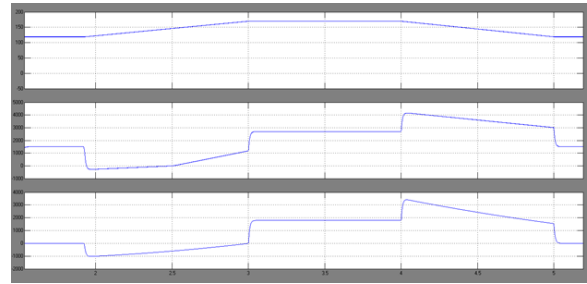
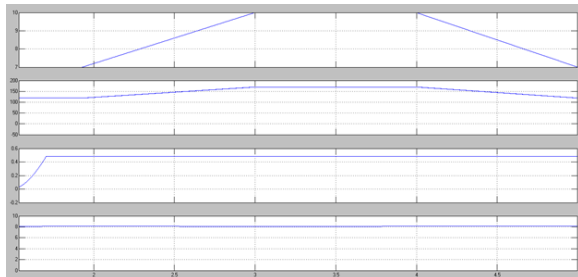
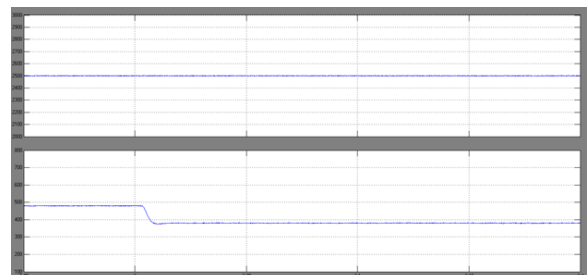
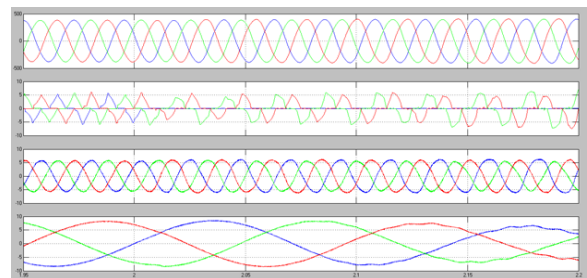


Fig. 10. Dynamic performance of DFIG based WPGS with BES for wide span of wind speed variation (a)  $V_w$ ,  $\dot{u}_r$ ,  $C_p$ ,  $\ddot{e}^*$ ,  $v_{sa}$ ,  $i_{sa}$ ,  $i_{rabc}$  (b)  $\dot{u}_r$ ,  $P_s$ ,  $PLSC$ ,  $P_b$ ,  $V_t$ ,  $f_s$ .



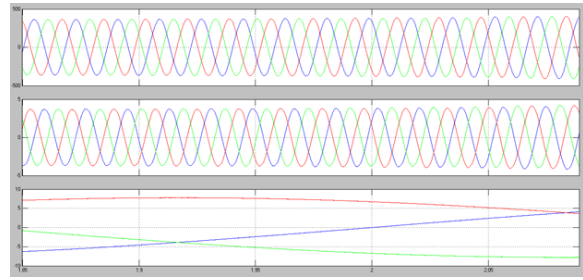
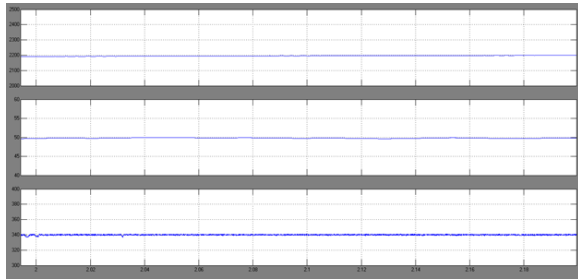
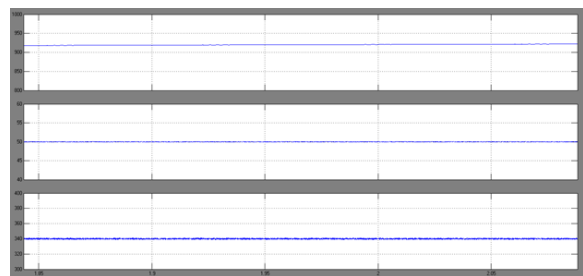
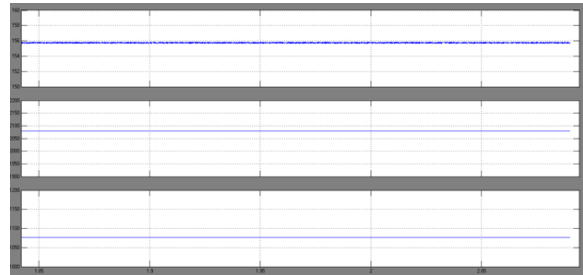
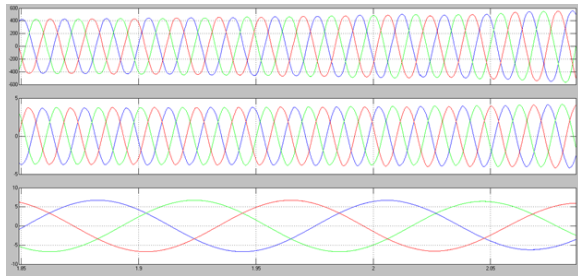


Fig. 11. Non-linear unbalancing mechanism dynamic response:  $v_{sabc}$ ,  $i_{Labc}$ ,  $i_{sabc}$ ,  $i_{rabc}$ ,  $P_s$ ,  $P_L$ ,  $P_b$ ,  $V_t$ ,  $f_s$ .

**Simulation results with genetic algorithm:**



(b) 9.23 m/s (synchronous speed of DFIG):  $v_{sabc}$ ,  $i_{sabc}$ ,  $i_{rabc}$ ,  $\omega_r$ ,  $P_s$ ,  $PLSC$ ,  $P_b$ ,  $V_t$ ,  $f_s$ .

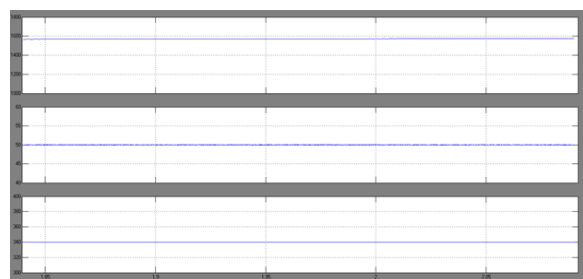
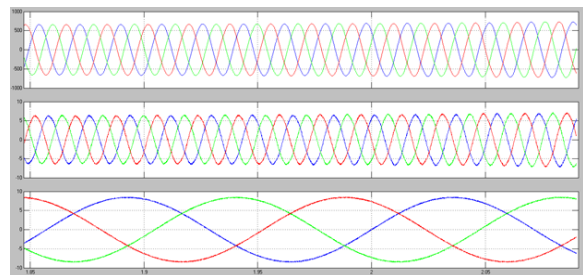
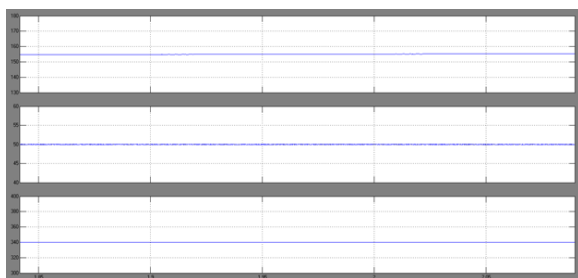
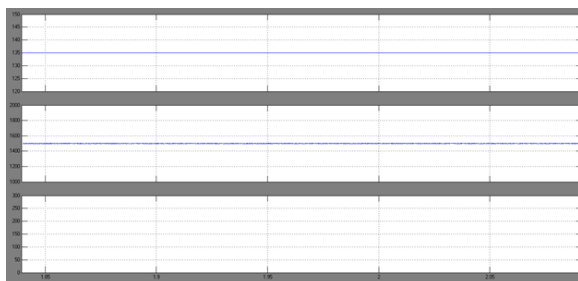


Fig. 8. Performance of the DFIG based WPGS with BES at constant wind speed of (a) 8 m/s (subsynchronous speed of DFIG):  $v_{sabc}$ ,  $i_{sabc}$ ,  $i_{rabc}$ ,  $\omega_r$ ,  $P_s$ ,  $PLSC$ ,  $P_b$ ,  $V_t$ ,  $f_s$

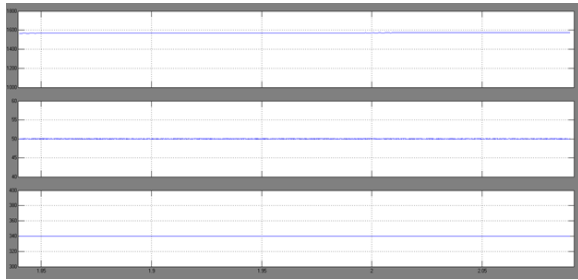
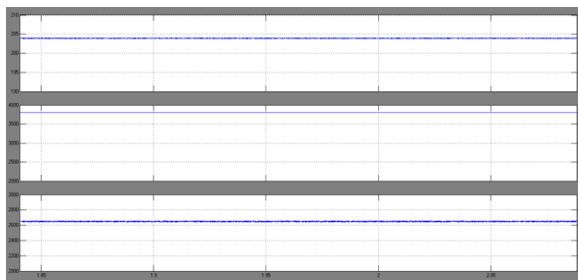
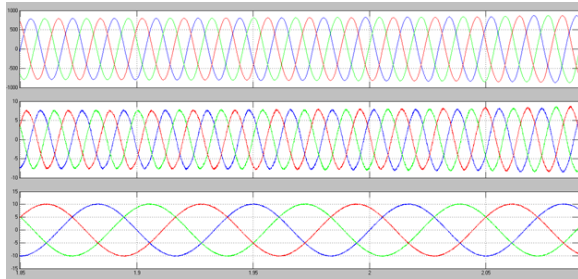


Fig. 9. Performance of the DFIG based WPGS with BES at constant wind speed of (a) 10 m/s (supersynchronous speed of DFIG):  $v_{sabc}$ ,  $i_{sabc}$ ,  $i_{rabc}$ ,  $\omega_r$ ,  $P_s$ ,  $PLSC$ ,  $P_b$ ,  $V_t$ ,  $f_s$



(b) 12 m/s (supersynchronous speed of DFIG):  $v_{sabc}$ ,  $i_{sabc}$ ,  $i_{rabc}$ ,  $\omega_r$ ,  $P_s$ ,  $PLSC$ ,  $P_b$ ,  $V_t$ ,  $f_s$ .

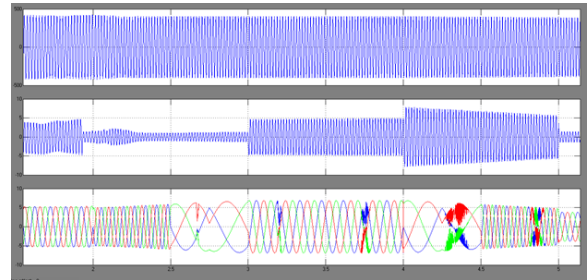
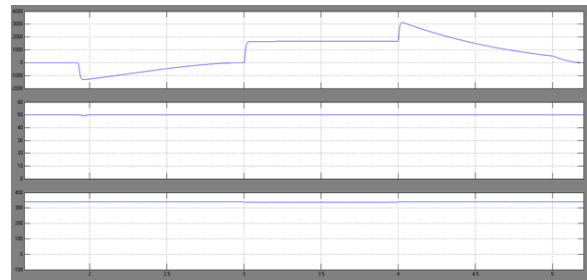
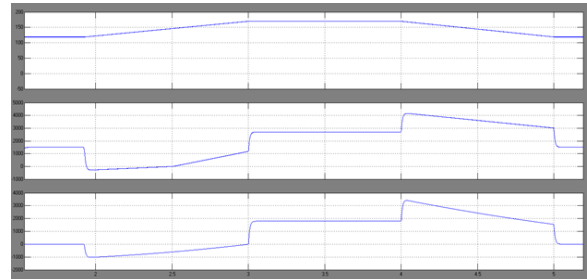
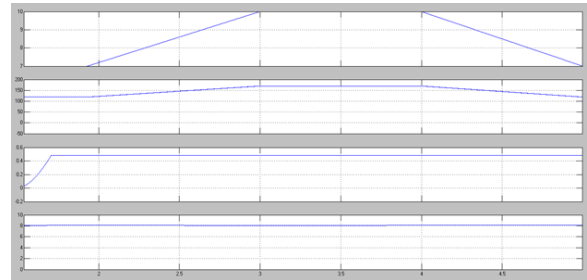
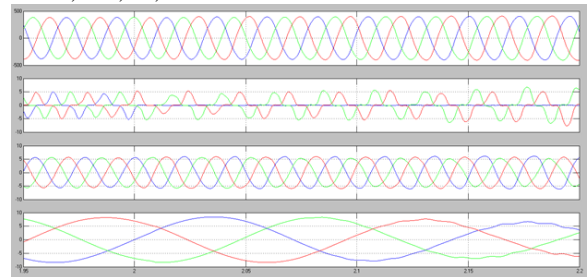


Fig. 10. Dynamic performance of DFIG based WPGS with BES for wide span of wind speed variation (a)  $V_w$ ,  $\dot{u}_r$ ,  $C_p$ ,  $\ddot{e}^*$ ,  $v_{sa}$ ,  $i_{sa}$ ,  $i_{rabc}$  (b)  $\dot{u}_r$ ,  $P_s$ ,  $PLSC$ ,  $P_b$ ,  $V_t$ ,  $f_s$ .



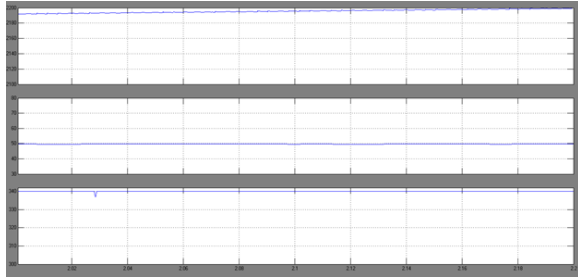


Fig. 11. Dynamic response of the system for nonlinear unbalancing load : vsabc, iLabc, isabc, irabc, Ps, PL, Pb, Vt, fs.

### CONCLUSION

A single information variable FLC based control has been proposed for DFIG based WPGS in free mode. This FLC is utilized to tune contrasting and essential controllers increases as shown by the spoil segments with a definitive target that MPPT is followed enough by and large under extraordinary working conditions. The BES is used for storing the centrality of fulfilment when the demand heap is not really of age and, in addition, the levelling capacity when the demand heap is above age. The huge achievements using the proposed control are shown as follows.

- The stator voltages and streams are sinusoidal and are modified at an extremely fundamental level in proximity to nonlinear and unequal weight conditions.
- Unmistakably high force extraction from the variable breeze velocity is sufficiently refined in a low and large combination of wind speeds.
- DFIG-based WPGS terminal voltage and rehazarding are continuous wind speed combinations self-regulation.

Reenacted data show that the system also operates for non-linear imbalance at variable breeze speeds. Irrefutably the symphonious dashes of stator voltages and stator streams, are found inside the IEEE 519 norm. Moreover, exploratory outcomes have demonstrated the appealing execution of the introduced structure.

### REFERENCES

1] M. Marchi, V. Niccolucci, R. M. Pulselli, and N. Marchettini, Environmental policies for GHG emissions reduction and energy transition in the

medieval historic centre of Siena (Italy): the role of solar energy, *Journal of Cleaner Production*, vol. 185, pp. 829-840, 2018.

[2] P. Haan, M. Simmler, Wind electricity subsidies- A windfall for landowners? Evidence from a feed-in tariff in Germany, *Journal of Public Economics*, vol. 159, pp. 16-32, 2018.

[3] W. Li, P. Chao, X. Liang, J. Ma, D. Xu, and X. Jin, A practical equivalent method for DFIG wind farms, *IEEE Trans. Sustain. Energy*, vol. 9, no. 2, pp. 610-620, Sept. 2018.

[4] T. Malakar, S.K. Goswami, and A.K. Sinha, Impact of load management on the energy management strategy of a wind-short hydro hybrid system in frequency based pricing, *Energy Convers. and Manage.*, vol 79, pp. 200-212, March 2014.

[5] V. Gholamrezaie, M. G. Dozein, H. Monsef, and B. Wu, An optimal frequency control method through a dynamic load frequency control (LFC) model incorporating wind farm, *IEEE Systems Journal*, vol. 12, no. 1, pp. 392-401, March 2018.

[6] H. Li and Z. Chen, "Overview of different wind generator systems and their comparisons," *IET Renewable Power Generation*, vol. 2, no. 2, pp.

123-138, June 2008.

[7] C. Wu and H. Nian, "Stator harmonic currents suppression for DFIG based on feed-forward regulator under distorted grid voltage," *IEEE Trans. Power Electron.*, vol. 33, no. 2, pp. 1211-1224, Feb. 2018.

[8] C. Cheng and H. Nian, "Low-complexity model predictive stator current control of DFIG under harmonic grid voltages," *IEEE Trans. Energy Convers.*, vol. 32, no. 3, pp. 1072-1080, Sept. 2017.

[9] D. Sun, X. Wang, H. Nian, and Z. Q. Zhu, "A sliding-mode direct power control strategy for DFIG under both balanced and unbalanced grid conditions using extended active power," *IEEE Trans. Power Electron.*, vol. 33, no. 2, pp. 1313-1322, Feb. 2018.

[10] I. D. Margaritis, S. A. Papathanassiou, N. D. Hatziargyriou, A. D. Hansen, and P. Sorensen, "Frequency control in autonomous power systems with high wind power penetration," *IEEE Trans. Sustain. Energy*, vol. 3, no. 2, pp. 189-199, April 2012.



INTERNATIONAL JOURNAL OF ADVANCED RESEARCH  
IN COMPUTER SCIENCE AND ENGINEERING TECHNOLOGIES

**ISSN 2454-9924**